Noncoherent detection of DQPSK in OFDM systems using predictive VA

Vineel K Veludandi and K Vasudevan

Department of Electrical Engineering, IIT Kanpur, 208016, Kanpur, India

Email: vineelkv@iitk.ac.in, vasu@iitk.ac.in .

Abstract. Noncoherent detection of differential quaternary phase shift keying (DQPSK) signals in OFDM systems is efficiently implemented using a predictive Viterbi algorithm (VA) operating on a trellis with just $S_T = M^{P-1}$ states instead of M^P states, where M denotes an M-ary PSK constellation and P denotes the order of the prediction filter. The prediction filter coefficients are generated based on the channel DFT alone making a high SNR approximation, since the estimation of the noise-variance using training symbols results in loss of throughput.

1. Introduction

Orthogonal Frequency Division Multiplexing (OFDM) is a spectrally efficient, discrete-time implementation of the multicarrier communication system [1]. Data detection in OFDM systems can be performed in three ways. They are

- Coherent detection [2, 3] which require the estimate of the channel impulse response.
- Suboptimal ML detection [4] which require the statistics of the channel fade process.
- Noncoherent detection [5] which does not require any knowledge of the channel fade process nor its statistics.

Channel fade process and its statistics are estimated using training symbols embedded into the OFDM frame [6]. Channel and statistics estimation using training symbols results in loss of throughput and hence the need for noncoherent detection. In [5], predictive VA is used for detecting 8-PSK in Rayleigh flat-fading channel, whereas in this paper, predictive VA is used for detecting DQPSK in OFDM systems. Perfect carrier and timing synchronization is assumed.

A high degree of correlation in the channel frequency response is obtained at the output of FFT, when the channel memory is much less than FFT length. The proposed predictive VA-based receiver exploits this correlation using a linear prediction filter for decorrelating the channel frequency response. There are M^P ways in which a prediction filter of order P can be populated. However, in [5], the complexity of the trellis is reduced to M^{P-1} states, using the concept of isometry.

2. Notation

In this paper, all lower-case and upper-case letters without a tilde e.g., g_k represent real-valued scalars. Letters with a tilde e.g., $\tilde{h}_k$, denote complex quantities. However, complex data symbols are denoted by S_k (without a tilde). Boldface letters represent vectors or matrices. The $(.)^{\mathcal{H}}$ denotes conjugate transpose, $(.)^T$ denotes transpose and $E[.]$ denotes the expectation operation.

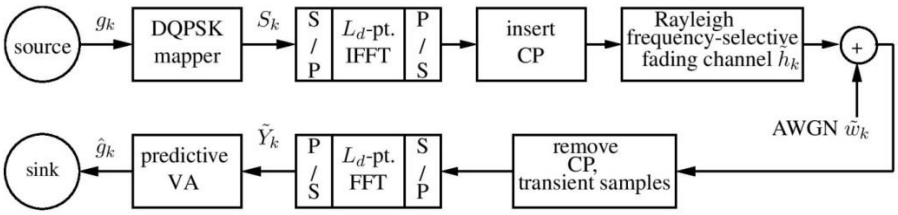

Figure 1: System model. Two consecutive bits of $\boldsymbol{g_k}$ are mapped to QPSK using the differential encoding rules in Table 1.

3. System Model

The block diagram of the system is given in Figure 1. The binary input data g_k $(0 \le k \le 2L_d - 1)$ is mapped to differential quadrature shift keying (DQPSK) to get S_k $(0 \le k \le L_d - 1)$ according to the differential encoding rules given in Table 1 [1].

Table 1: Differential encoding rules

Dibit $(g_{k-1}g_k)$	Phase change (in radians)
00	0
01	$\pi/2$
10	$3\pi/2$
11	π

The symbol stream S_k is modulated onto the orthogonal subcarriers by an L_d-point IFFT operation. A cyclic prefix (CP) of length $L_h - 1$ is inserted in the time domain to convert linear convolution with the Rayleigh frequency selective fading channel $\tilde{h}_k$ $(0 \le k \le L_h - 1)$ into a circular convolution [1].

The channel coefficients are $\tilde{h}_k \sim \mathcal{CN}(0, 2\sigma_f^2)$ are independent over time k in each OFDM frame, that is,

$$0.5 \times E\left[\tilde{h}_k \tilde{h}_{k-m}^*\right] = \sigma_f^2 \delta_K(m) \tag{1}$$

where $\delta_K(.)$ denotes the Kronecker delta function and also varies independently from frame to frame, that is, quasistatic. The AWGN samples $\tilde{w}_k \sim \mathcal{CN}(0, 2\sigma_w^2)$ $(0 \le k \le L_d - 1)$ are independent over time k in each OFDM frame, that is,

$$0.5 \times E[\tilde{w}_k \tilde{w}_{k-m}^*] = \sigma_w^2 \delta_K(m) \tag{2}$$

and also varies independently from frame to frame.

4. Receiver

The received samples at the FFT output are given by (for $0 \le k \le L_d - 1$)

$$\tilde{Y}_k = \tilde{H}_k S_k + \tilde{W}_k, \text{ where } \tilde{H}_k = \sum_{i=0}^{L_h-1} \tilde{h}_i e^{-j2\pi ik/L_d}, \tilde{W}_k = \sum_{i=0}^{L_d-1} \tilde{w}_i e^{-j2\pi ik/L_d}. \tag{3}$$

The autocorrelation of the channel DFT is given by [3]

$$\tilde{R}_{\tilde{H}\tilde{H},m} \triangleq 0.5 \times E\left[\tilde{H}_k \tilde{H}_{k-m}^*\right] = \sigma_f^2 \sum_{n=0}^{L_h-1} e^{-j2\pi nm/L_d}. \tag{4}$$

Now consider $\tilde{X}_k = \tilde{Y}_k / S_k \approx \tilde{H}_k$ (at high SNR). The autocorrelation of the $\tilde{X}_k$ is given by

$$\tilde{R}_{\tilde{X}\tilde{X},m} = \tilde{R}_{\tilde{H}\tilde{H},m} + (\sigma_w^2 L_d \delta_K(m) / |S_k|^2). \tag{5}$$

In practice, the prediction filter coefficients are generated using the autocorrelation in (5) which is estimated with the help of training symbols. However, in this paper, the prediction filter coefficients are generated from (4).

Note that the detection rule for the ideal coherent receiver is

$$\hat{S}_k = \min_{S_k} \left| \tilde{Y}_k - \tilde{H}_k S_k \right|^2. \tag{6}$$

4.1 Noncoherent Detection Principle [5]

In this subsection we give the principle of the operation for the proposed predictive VA-based receiver. The received samples can be represented in matrix form as

$$\widetilde{\mathbf{Y}} = \mathbf{S}^{(q)}\widetilde{\mathbf{H}} + \widetilde{\mathbf{W}},\ 0 \le q \le M^{L_d} - 1 \tag{7}$$

where $\widetilde{\mathbf{Y}}$ is an $L_d \times 1$ matrix of received samples, $\mathbf{S}^{(q)}$ is an $L_d \times L_d$ matrix with elements containing the q^{th} possible transmitted DQPSK symbol sequence, $\widetilde{\mathbf{H}}$ is an $L_d \times 1$ matrix of the channel DFT and $\widetilde{\mathbf{W}}$ an $L_d \times 1$ matrix containing the DFT of the AWGN samples $\widetilde{w}_k$.

The noncoherent ML detector decides in favour of $\mathbf{S}^{(q)}$ that maximizes the conditional probability density function $p(.)$ as

$$\max_q\ p\left(\widetilde{\mathbf{Y}}\ |\mathbf{S}^{(q)}\right)\ \Rightarrow\ \max_q \exp\left(-\frac{1}{2}\widetilde{\mathbf{Y}}^{\mathcal{H}}\left(\widetilde{\boldsymbol{R}}^{(q)}\right)^{-1}\widetilde{\mathbf{Y}}\right), \text{ where}$$

$$\widetilde{\boldsymbol{R}}^{(q)} \triangleq \frac{1}{2}E\left[\widetilde{\mathbf{Y}}\,\widetilde{\mathbf{Y}}\ |\mathbf{S}^{(q)}\right] = \frac{1}{2}\mathbf{S}^{(q)}E\left[\widetilde{\mathbf{H}}\,\widetilde{\mathbf{H}}^{\mathcal{H}}\right]{\mathbf{S}^{(q)}}^{\mathcal{H}} + \sigma_w^2 L_d\mathbf{I}\ \approx \frac{1}{2}\mathbf{S}^{(q)}E\left[\widetilde{\mathbf{H}}\,\widetilde{\mathbf{H}}^{\mathcal{H}}\right]{\mathbf{S}^{(q)}}^{\mathcal{H}} = \frac{1}{2}\mathbf{S}^{(q)}\boldsymbol{\Phi}{\mathbf{S}^{(q)}}^{\mathcal{H}} \tag{8}$$

Note that $\widetilde{\boldsymbol{R}}^{(q)}$ is not a diagonal matrix, since channel DFT is highly correlated. Using Cholesky factorization of the autocovariance matrix, it can be shown that $\boldsymbol{\Phi}^{-1} = \widetilde{\mathbf{B}}^{\mathcal{H}}\mathbf{D}^{-1}\widetilde{\mathbf{B}}$, where

$$\widetilde{\mathbf{B}} \triangleq \begin{bmatrix} 1 & 0 & \dots & 0 \\ \tilde{a}_{1,1} & 1 & \dots & 0 \\ \vdots & \vdots & \vdots & \vdots \\ \tilde{a}_{L_d-1,L_d-1} & \tilde{a}_{L_d-1,L_d-2} & \dots & 1 \end{bmatrix}, \qquad \mathbf{D} \triangleq \begin{bmatrix} \sigma_0^2 & \dots & 0 \\ \vdots & \ddots & \vdots \\ 0 & \dots & \sigma_{L_d-1}^2 \end{bmatrix}. \tag{9}$$

$\widetilde{\mathbf{B}}$ is the $L_d \times L_d$ matrix of predictor coefficients with $\tilde{a}_{i,\tau}$ being the τ^{th} coefficient of the optimum i^{th} −order predictor and $\mathbf{D}$ is the $L_d \times L_d$ matrix where σ_k^2 is the 1-D prediction error variance of the k^{th} −order predictor (minimum mean square-error sense). The prediction coefficients are generated using Levinson-Durbin algorithm based on the autocorrelation of the channel DFT given in (4).

The maximization rule in (8) can be simplified as

$$\min_q \widetilde{\mathbf{Y}}^{\mathcal{H}}\left(\left(\mathbf{S}^{(q)}\right)^{\mathcal{H}}\right)^{-1}\widetilde{\mathbf{B}}^{\mathcal{H}}\mathbf{D}^{-1}\widetilde{\mathbf{B}}\left(\mathbf{S}^{(q)}\right)^{-1}\widetilde{\mathbf{Y}}\ \Rightarrow \min_q\left(\sum_{k=0}^{P-1}\frac{\left|\tilde{z}_k^{(q)}\right|^2}{2\sigma_k^2} + \sum_{k=P}^{L_d-1}\frac{\left|\tilde{z}_k^{(q)}\right|^2}{2\sigma_k^2}\right) \tag{10}$$

where $$\left[\tilde{z}_0^{(q)}\ \tilde{z}_1^{(q)}\ \dots\ \tilde{z}_{L_d-1}^{(q)}\right]^T \triangleq \tilde{\mathbf{z}}^{(q)} = \widetilde{\mathbf{B}}\left(\mathbf{S}^{(q)}\right)^{-1}\widetilde{\mathbf{Y}}. \tag{11}$$

The first part of the summation in (10) represents the transient-part and the second-part represents the steady-state. In this paper, we only consider the steady-state part. Assuming that a P^{th} −order predictor completely decorrelates the fade process, the final decision rule can be given as

$$\min_q \sum_{k=P}^{L_d-1}\left|\tilde{z}_k^{(q)}\right|^2,\ \text{where}\quad \tilde{z}_k^{(q)} = \sum_{i=0}^{P}\tilde{a}_{P,i}\tilde{Y}_{k-i}/S_{k-i}^{(q)}. \tag{12}$$

The complexity in (12) increases exponentially with message length L_d. However (12) can be efficiently implemented using a predictive VA algorithm.

4.2 Trellis Construction [1]

In this section, we assume that the DQPSK mapper in Figure 1 is not present. In section 4.3, we motivate the need for the DQPSK mapper. Assume that the n bits from the source are mapped to an M-ary ($M = 2^n$) constellation according to the mapping $S = \mathcal{M}(.)$. Here, $\mathcal{S}_{j,0}$ ($0 \le \mathcal{S}_{j,0} \le 2^n - 1$) is the decimal equivalent of the n bits $g_k g_{k-1} g_{k-2} \cdots g_{k-n+1}$ in Figure 1, and is referred to as the input digit. The number of states in the trellis would be $S_T = M^P$, since there are M^P ways in which a prediction filter of order P can be populated.

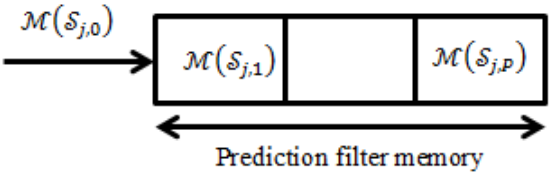

Figure 2: Procedure for constructing trellis.

Note that $\{\mathcal{M}(\mathcal{S}_{j,0}), \mathcal{M}(\mathcal{S}_{j,1}), \dots, \mathcal{M}(\mathcal{S}_{j,P})\}$ in Figure 2 refers to one of the paths in the trellis. The j^{th} trellis state can be represented by a *M*-ary *P* tuple as $\mathcal{S}_j$: $\{\mathcal{S}_{j,1} \dots \mathcal{S}_{j,P}\}$ for $0 \le j \le M^P - 1$ where $\mathcal{S}_{j,k} \in \{0, \dots, M-1\}$.

Given the present state $\mathcal{S}_j$ and input $\mathcal{S}_{j,0}$ ($\mathcal{S}_{j,0} \in \{0, \dots, M-1\}$), the next state is given by $\mathcal{S}_i$: $\{\mathcal{S}_{j,0}\, \mathcal{S}_{j,1} \dots \mathcal{S}_{j,P-1}\}$, that is, right-shift operation.

4.3 Complexity reduction of the trellis using isometry [5]

Replacing $\mathbf{S}^{(q)}$ by $\mathbf{S}^{(q)}e^{j\phi}$ (here ϕ refers to constant phase) in (8) will yield the same metric in (12) (isometry problem) and this problem can be solved by differential encoding.

Consider the error signal in (12), which is,

$$\tilde{z}_k^{(q)} = \sum_{i=0}^{P} \tilde{a}_{P,i} \tilde{Y}_{k-i} / S_{k-i}^{(q)} = 1/S_k{}^{(q)} \sum_{i=0}^{P} \tilde{a}_{P,i} \tilde{Y}_{k-i} S_k{}^{(q)} / S_{k-i}^{(q)}. \quad (13)$$

It can be observed that $\left|\tilde{z}_k^{(q)}\right|^2$ is independent of $S_k{}^{(q)}$ (isometry) and is dependent only on the phase changes between $S_k{}^{(q)}$ and $S_{k-1}{}^{(q)} \dots S_{k-P}{}^{(q)}$. That is, $S_k{}^{(q)}/S_{k-P}{}^{(q)} = f(\mathcal{S}_{j,0}\mathcal{S}_{j,1} \dots \mathcal{S}_{j,P-1})$ where $f(.)$ is some function of input digits $\mathcal{S}_{j,0}\mathcal{S}_{j,1} \dots \mathcal{S}_{j,P-1}$ depending on the differential encoding rules given in Table 1. This suggests that the contents of the prediction filter can always be represented with an unity as its first element. Now, the number of states in the normalized trellis (that is, with differential encoding) required for a P^{th}-order predictor would be only $S_T = M^{P-1}$.

4.4 Predictive VA algorithm [1]

The predictive VA operates on the normalized trellis. Let $\mathcal{C}_n$ denote the states that converge to the state *n* ($0 \le n \le S_T - 1$). Let $\mu_{i,n}$ denote the path metric at time instant *i* ($0 \le i \le L_d$) and state *n*. Let $\nu_{i,m,n}$ denote the branch metric at time instant *i* corresponding to the transition from state *m* to state *n* and is given as

$$\nu_{i,m,n} = \left|\sum_{j=0}^{P} \tilde{a}_{P,j} \tilde{Y}_{i-j} / S_{j,m,n}\right|^2 \quad (14)$$

where $S_{0,m,n}$ denote the input symbol corresponding to the transition from state *m* to *n* and the data $S_{j,m,n}$ are the contents of the prediction filter of state *m*. The algorithm is as follows:

(i) Now set initial values as $i = 0$ and $\mu_{0,n} = 0$ (for $0 \le n \le S_T - 1$), since the receiver does not know the starting state.

(ii) Increase time *i* by 1

(a) Compute the path metrics at each state *n* as $\mu_{i,n} = \min_{m \in \mathcal{C}_n} \{\nu_{i,m,n} + \mu_{i-1,m}\}$.

(b) Store the survivor for each state *n*.

(c) Having the minimum path metric, trace back along the survivor path and release a symbol corresponding to time $i - \mathcal{D}_V$, where $\mathcal{D}_V$ is the decoding delay of VA.

(iii) Repeat step 4.4.2 until time $i = L_d$.

5. Results

5.1 SNR parameters

Since the overall rate is 2, the SNR per bit is defined as [3]:

$$\text{SNR per bit} = 0.5 \times E\left[\left|\widetilde{H}_k S_k\right|^2\right] / E\left[\left|\widetilde{W}_k\right|^2\right] = 0.5 \times \left(L_h \times 2\sigma_f^2\right) \times E[|S_k|^2] / (L_d \times 2\sigma_w^2). \quad (15)$$

In Figure 3, we compare the proposed predictive VA-based receiver for different values of prediction orders. In Figure 4, we give the performance of the ideal predictive VA-based detector for different values of P. Note that in Figure 4, the prediction coefficients are generated based on both the channel DFT and the noise, that is using (5) assuming that the receiver has the perfect knowledge of the noise-variance.

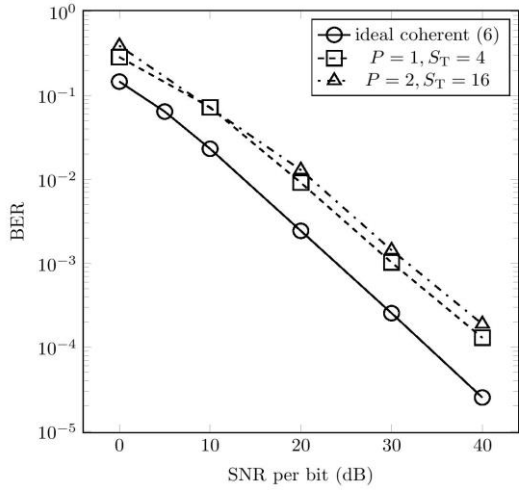

Figure 3: BER performance of the proposed predictive VA-based receiver for $L_d = 1024$, $\sigma_f^2 = 0.5$ and $L_h = 10$ using the predictor coefficients obtained from $\tilde{R}_{\tilde{H}\tilde{H},m}$ in (4).

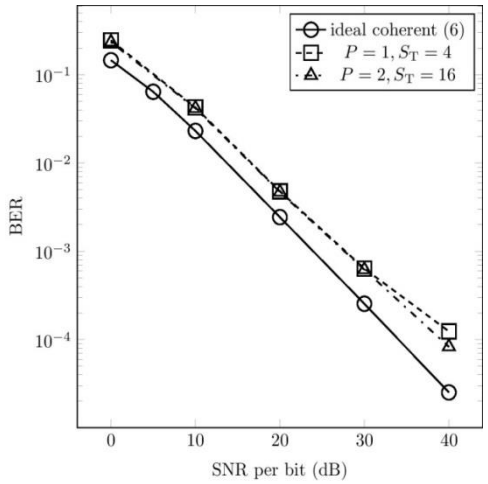

Figure 4: BER performance of the ideal predictive VA-based receiver for $L_d = 1024$, $\sigma_f^2 = 0.5$ and $L_h = 10$ using the predictor coefficients obtained from $\tilde{R}_{\tilde{H}\tilde{H},m}$ in (5)

6. Conclusion

Simulation results show that the performance of the proposed method is as good as the ideal predictive VA-based receiver. The proposed approach is perfectly suitable for applications which demand high throughput, since the proposed detection method is without channel estimation which requires training symbols. Future work can be focussed on incorporating error correcting codes to reduce the transmit power.

References

[1] Vasudevan K 2007 *Digital Communications and Signal Processing* (Hyderabad: Universities Press)

[2] Vasudevan K 2015 Coherent detection of turbo-coded ofdm signals transmitted through frequency selective fading channels with receiver diversity and increased throughput *Wireless Personal Communications* **82** 1623-42

[3] Vasudevan K 2013 *IEEE Int. Conf. on Signal Processing Computing and Control* (Shimla) pp 26-28

[4] Sanzi F, Jelting S and Speidel J 2003 A comparative study of iterative channel estimators for mobile ofdm systems *IEEE Transactions on Wireless Communications* **2** 849-59

[5] Vasudevan K, Giridhar K and Ramamurthi B 2001 Efficient suboptimum detectors based on linear prediction in Rayleigh flat-fading channels *Signal Processing Journal* **81** 819-28

[6] Coleri S, Ergen M, Puri A and Bahai A 2002 Channel estimation techniques based on pilot arrangement in ofdm systems *IEEE Transactions on Broadcasting* **48** 223-29.